Energy Conversion and Management 65 (2013) 26–32

Contents lists available at SciVerse ScienceDirect

Energy Conversion and Management

journal homepage: www.elsevier.com/locate/enconman

The thermoelement as thermoelectric power generator: Effect of leg geometry on the efficiency and power generation

Ahmet Z. Sahin *, Bekir S. Yilbas

Mechanical Engineering Department, King Fahd University of Petroleum and Minerals, Dhahran, Saudi Arabia

ARTICLE INFO

Article history:
Received 7 December 2010
Received in revised form 17 July 2012
Accepted 24 July 2012
Available online 11 October 2012

Keywords:
Thermoelectric
Power
Leg geometry
Efficiency
Constructal design

ABSTRACT

Thermoelectric power generators are one of the promising clean energy resources with the cost effective operation despite the low device efficiency. Investigation into device efficiency improvement is necessary for the practical applications. Consequently, in the present study, a theoretical analysis of thermoelectric power generator is carried out and influence of thermoelectric leg geometry on the device efficiency and the power generation is formulated. The geometric configuration of the legs in the device is associated with the shape parameter and incorporated in the analysis. The influence of the shape parameter on the device efficiency and power generation is examined for various temperature and external load resistance ratios. It is found that increasing or decreasing of the shape parameter (μ) has a favorable effect on the device efficiency; however, the shape parameter (μ) has an adverse effect on the thermoelectric power generation.

1. Introduction

The requirement of clean energy and the technological developments lead to extensive research into the renewable energy resources. One of the promising clean energy sources is the thermoelectric power generators. Since these devices do not have the moving parts, the operation and maintenance of thermoelectric power generators are easy and less costly. The efficiency of thermoelectric generator is highly depending on the operating temperatures, the figure of merit, and design configuration including the external load parameter of the device. In most of the power generation applications, the figure of merit is on the order of 1 resulting in low device thermal efficiency. Although the research into thermoelectric material development for high figure of merit is progressing, the maximum device thermal efficiency is still on the order of less than 10%. Since the design configuration including geometric arrangements of the thermoelectric legs influences the thermal efficiency, investigation into leg geometry on the thermoelectric power generation and the device thermal efficiency becomes essential. Many aspects of thermoelectrics including energy conversion, performance optimization, thermoelectric material characterization, and various applications have been studied extensively in the literature [1–14].

Considerable research studies were also carried out to examine thermoelectric power generation and device efficiency. Design and thermal analysis of solar thermoelectric power generation system were carried out by Vatcharasathien et al. [15]. They considered truncated parabolic collectors with a flat receiver, conventional flat-plate collectors, and thermoelectric power generator modules in the performance analysis. The optimization study for the waste heat thermoelectric generator system was carried out by Gou et al. [16]. They indicated that the promising potential was present to use a thermoelectric generator for a low-temperature waste heat recovery, especially in the industrial fields. The system performance of the thermoelectric generator was investigated by Xiao et al. [17]. They introduced a mathematical model for the thermoelectric generator performance using the finite time thermodynamic analysis. Thermoelectric power conversion from heat re-circulating combustion systems was examined by Weinberg et al. [18]. The findings revealed that the efficiency of thermoelectric devices could be improved for certain arrangements of the locations of the devices around the heat transferring surface. The model study in relation to design of a thermoelectric power generator maximizing the performance of the device was carried out by Crane and Bell [19]. They introduced the gradient based optimization technique to incorporate the interactions between various design variables and parameters for the optimal design to maximize the performance. A physical model for thermoelectric generators was introduced by Freunek et al. [20]. They presented geometric optimization and investigated the influence of Peltier heat leak conditions and load resistance on the thermoelectric power generation. The performance analysis of a two-stage thermoelectric generator was carried out by Chen et al. [21]. In the analysis, the fixed total number of thermoelectric elements of the combined device is considered and the allocations of the thermoelectric element pairs

* Corresponding author.
E-mail address: azsahin@kfupm.edu.sa (A.Z. Sahin).

0196-8904/$ - see front matter © 2012 Elsevier Ltd. All rights reserved.
http://dx.doi.org/10.1016/j.enconman.2012.07.020

Nomenclature

A	area (m^2)
I	electrical current (A)
k	thermal conductivity (W/mK)
K	overall thermal conductance of the thermoelectric generator (W/K)
L	length (height) of leg (m)
Q	heat flux (W)
R	overall electrical resistance of the thermoelectric generator (Ω)
R_L	external load resistance (Ω)
s	shape parameter of leg, dA/dx (m)
T	temperature (K)
W	power output (W)
Z	figure of merit (1/K)
α	seebeck coefficient (V/K)
μ	dimensionless shape parameter (Eq. (22))
η	efficiency
σ	electrical conductivity (1/Ωm)
θ	temperature ratio (T_2/T_1)

among the two thermoelectric generators as well as the two thermoelectric heat pumps were optimized for maximizing the heat load and the coefficient of performance. The simulation study for thermoelectric power generation with multi-panels was carried out by Suzuki and Tanaka [22]. They indicated that the proper arrangements of the thermoelectric panels could shorten significantly the device area despite the fact that the output from the multi-panels could decrease a few percent. The solar thermoelectric generator for micro-power applications was investigated by Amatya and Ram [23]. They presented a thermodynamic analysis for predicting the thermal-to-electric conversion efficiency of the generator.

Although thermodynamic analysis of thermoelectric devices pertinent to the performance assessment has been presented extensively in the open literature [24–38], the influence of the geometric configuration of the thermoelectric device legs on the device performance is left obscure. Some of the earlier works [30,39,40] that consider the effect of the geometry on the performance of thermoelectric elements do not take into account the effect of geometry on the current that flows through the device. Consequently, in the present study the influence of thermoelectric device leg geometry on the power generation and the thermal efficiency that belongs to domain of "constructal design" [41] is examined. The theoretical analysis incorporating the operating parameters such as temperature ratio, external load, and device resistance, is presented. The functional relation between the thermoelectric power generation and the leg geometric parameter, namely shape parameter, is developed. The study is extended to include the efficiency analysis incorporating the leg shape parameter.

2. Thermal analysis

Consider the thermoelectric element of variable cross section shown in Fig. 1. The properties of leg material are assumed to be constant (no temperature or position dependence of the material properties, e.g. Seebeck coefficient, thermal and electrical conductivity) so the Thomson effect is inherently neglected. In addition, we assume no heat losses due to radiation and convection, no contacts (and contact resistances) and no external irreversibilities (transfer from heat sources) in the calculation. The calculation is in steady-state and based on a (quasi)-one dimensional approach. We use Dirichlet boundary conditions. Thus the efficiency of the thermoelectric power generator with legs of variable cross-section, which is shown in Fig. 1 is given as

$$\eta = \frac{I^2 R_L}{\alpha I T_1 + K(T_1 - T_2) - \frac{1}{2} I^2 R} \tag{1}$$

where K is the thermal conductance and R is the electrical resistivity of the thermoelectric generator.

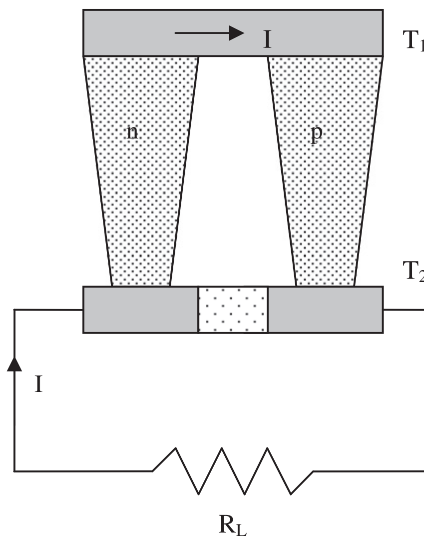

Fig. 1. Schematic view of a thermoelectric power generator with legs of variable cross-section.

The current I is a function of the net Seebeck coefficient $\alpha = \alpha_p - \alpha_n$ (the difference between the Seebeck coefficients of p and n junctions), the upper and lower junction temperatures (T_1 and T_2), the electrical resistance R and the external load resistance R_L as

$$I = \frac{\alpha(T_1 - T_2)}{R_L + R} \tag{2}$$

Substituting Eq. (2) in Eq. (1) the efficiency becomes

$$\eta = \frac{\alpha^2 (T_1 - T_2) R_L}{K(R_L + R)^2 + \alpha^2 T_1 (R_L + R) - \frac{1}{2}\alpha^2 (T_1 - T_2) R} \tag{3}$$

The cross-sectional area of the thermoelectric generator leg shown in Fig. 2 can be written as

$$A(x) = A_0 + \left(x - \frac{L}{2}\right) s \tag{4}$$

where A_0 is the average (mid-height) cross-sectional area, L is the height of the leg, and s is the shape parameter of the leg, i.e. rate of change of the cross-sectional area of the legs along the height direction

$$s = \frac{dA}{dx}$$

Considering the likely manufacturing complexities, the shape parameter s is assumed to be independent from x (i.e., the cross-sectional area of the legs are assumed to vary linearly along the height direction) in the present work.

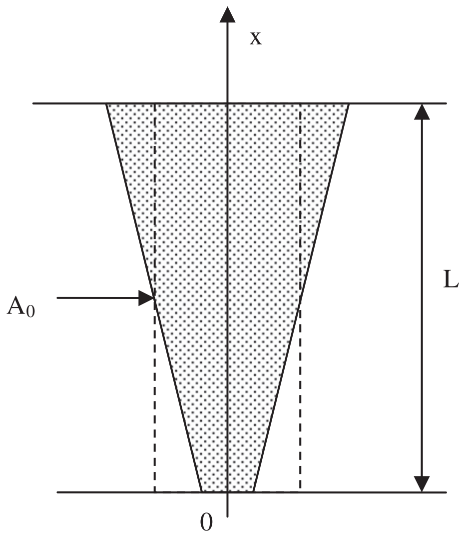

Fig. 2. Geometry of the thermoelectric generator leg.

The heat transfer rate through the leg along x is given by

$$\dot{Q} = -kA(x)\frac{dT}{dx} \tag{5}$$

After assuming a steady heating situation and isolated leg surfaces, Eq. (5) can be re-arranged as

$$\dot{Q}\int_0^L \frac{dx}{A(x)} = -k\int_{T_1}^{T_2} dT \tag{6}$$

Making use of Eq. (4) in Eq. (6), it and performing the integration

$$\dot{Q} = \frac{ks}{\ln\left(\frac{A_0+s\frac{L}{2}}{A_0-s\frac{L}{2}}\right)}(T_1 - T_2) \tag{7}$$

Eq. (7) indicates that the overall thermal conductance of the leg is

$$K_{\text{leg}} = \frac{ks}{\ln\left(\frac{A_0+s\frac{L}{2}}{A_0-s\frac{L}{2}}\right)} \tag{8}$$

Considering the two legs in Fig. 1, the total thermal conductance of the thermoelectric generator can be written as

$$K = \frac{(k_p + k_n)s}{\ln\left(\frac{A_0+s\frac{L}{2}}{A_0-s\frac{L}{2}}\right)} \tag{9}$$

where k_p and k_n are the thermal conductivities of the p-type and n-type legs, respectively.

On the other hand, the overall electrical resistance of the leg can be written as

$$R_{\text{leg}} = \int_0^L \frac{dx}{\sigma A(x)} \tag{10}$$

Substituting $A(x)$ from Eq. (4) and performing the integration, the overall electrical resistance is obtained as

$$R_{\text{leg}} = \frac{1}{\sigma s}\ln\left(\frac{A_0 + s\frac{L}{2}}{A_0 - s\frac{L}{2}}\right) \tag{11}$$

Similarly, considering the two legs the total electrical resistance of the thermoelectric generator becomes

$$R = \left(\frac{1}{\sigma_p} + \frac{1}{\sigma_n}\right)\frac{1}{s}\ln\left(\frac{A_0 + s\frac{L}{2}}{A_0 - s\frac{L}{2}}\right) = \frac{\sigma_p + \sigma_n}{\sigma_p\sigma_n s}\ln\left(\frac{A_0 + s\frac{L}{2}}{A_0 - s\frac{L}{2}}\right) \tag{12}$$

where σ_p and σ_n are the electrical conductivities of the p-type and n-type legs, respectively.

Substituting Eqs. (9) and (12) in Eq. (3) the efficiency of the thermoelectric generator can be written in dimensionless form as

$$\eta = (1-\theta) \times \frac{2ZT_{\text{ave}}\left(1+\sqrt{\frac{r_k}{r_\sigma}}\right)^2\left(\frac{R_L}{R_0}\right)}{(1+\theta)\left(\frac{K}{K_0}\right)\left(\frac{R_L}{R_0}+\frac{R}{R_0}\right)^2 + 2ZT_{\text{ave}}\left(1+\sqrt{\frac{r_k}{r_\sigma}}\right)^2\left[\frac{R_L}{R_0}+\frac{1}{2}\frac{R}{R_0}(1+\theta)\right]} \tag{13}$$

where

$$\theta = \frac{T_2}{T_1}, \quad (\text{Temperature ratio}) \tag{14}$$

$$r_k = \frac{k_p}{k_n}, \quad (\text{Thermal conductivity ratio}) \tag{15}$$

$$r_\sigma = \frac{\sigma_p}{\sigma_n}, \quad (\text{Electrical conductivity ratio}) \tag{16}$$

$$ZT_{\text{ave}} = \frac{\alpha^2\left(\frac{\sigma_n}{k_n}\right)T_1}{\left(1+\sqrt{\frac{r_k}{r_\sigma}}\right)^2}\left(\frac{1+\theta}{2}\right)$$

$$(\text{The figure of merit based on the average temperature}) \tag{17}$$

$$K_0 = \frac{A_0 k_n}{L} \quad (\text{Reference thermal conductance}) \tag{18}$$

and

$$R_0 = \frac{L}{A_0\sigma_n} \quad (\text{Reference electrical resistivity}) \tag{19}$$

Thus, the overall thermal conductance and overall electrical resistivity can be written in dimensionless form, respectively, as

$$\frac{K}{K_0} = \frac{\mu(r_k+1)}{\ln\left(\frac{1+\mu/2}{1-\mu/2}\right)} \tag{20}$$

and

$$\frac{R}{R_0} = \left(\frac{1+r_\sigma}{r_\sigma}\right)\frac{\ln\left(\frac{1+\mu/2}{1-\mu/2}\right)}{\mu} \tag{21}$$

where μ is the dimensionless shape parameter defined as

$$\mu = \frac{sL}{A_0} \tag{22}$$

On the other hand, the power generation from the thermoelectric power generator is given as

$$\dot{W} = I^2 R_L \tag{23}$$

or

$$\dot{W} = \frac{\alpha^2(T_1 - T_2)^2}{(R_L + R)^2}R_L \tag{24}$$

Thus the power generation can be written in dimensionless form as

$$\frac{\dot{W}}{K_0 T_2} = 2\frac{(1-\theta)^2}{\theta(1+\theta)}\frac{ZT_{\text{ave}}\left(1+\sqrt{\frac{r_k}{r_\sigma}}\right)^2\left(\frac{R_L}{R_0}\right)}{\left(\frac{R_L}{R_0}+\frac{R}{R_0}\right)^2} \tag{25}$$

Table 1
Experimental measurements of the figure of merit for Bi_2Te_3 thermoelectric material at room temperature (300 K) as reported in the literature.

Fabrication method	Figure of merit (*ZT*) at 300 K
Co-evaporation [42]	0.93
Co-sputtering [43]	0.31
Metalorganic chemical vapor deposition (MOCVD) [44]	0.98
Co-evaporation [45]	0.80
Electrochemical deposition (ECD) [46]	0.07
Flash evaporation [47]	0.53
Cu I added (patent) [48]	0.69

The following parameters have been used in the analysis:

$$\frac{R_L}{R_0} = 10,\ ZT_{\text{ave}} = 1.5,\ r_k = 1.0 \text{ and } r_\sigma = 1.0$$

Table 1 shows experimental measurements of the figure of merit for Bi_2Te_3 thermoelectric material fabricated using various methods. As can be seen from the table an average figure of merit of $ZT = 0.8$ can be considered to represent the figure of merit of Bi_2Te_3 thermoelectric generator at room temperature (i.e. at 300 K). However, in our analysis, the average temperature in the thermoelectric element is used to evaluate the figure of merit (ZT_{ave}). Therefore, a representative value of $ZT_{\text{ave}} = 1.5$ is taken in the present work. Eqs. (13) and (25) are used to compute the device efficiency and the power generation with the shape parameter for various temperature ratios and external resistance ratio.

3. Results and discussion

A theoretical analysis of thermoelectric power generator is carried out and influence of generator leg geometric configuration on the efficiency and the power generation is examined. The leg area along the leg height is considered to change linearly while assuming constant leg thickness along the leg height. The area variation along the leg height is incorporated in the analysis.

Fig. 3 shows variation of efficiency with the shape parameter ($\mu = sL/A_o$) for different temperature ratios ($\theta = T_2/T_1$). It should be noted that $\mu > 0$ represents the increasing leg area with increasing leg height while $\mu < 0$ corresponds to decreasing leg area with increasing leg height. Fig. 4 shows three-dimensional view of efficiency variation with the shape parameter and temperature ratio. Efficiency reduces with decreasing shape parameter (μ) and becomes minimum for the shape parameter $\mu = 0$, which corresponds to a rectangular leg geometry. The increase in the efficiency of the thermoelectric power generator is associated with overall electrical resistance of the leg (Eq. (11)), which reduces with increasing values of the shape parameter. It should be noted that the shape parameter can vary between negative and positive values depending on the shape of the leg geometry. Increasing the shape parameter from zero ($\mu > 0$), efficiency of the thermoelectric generator increases. This is, again, due to reducing overall electric resistance with increasing the shape parameter. Although efficiency of the thermoelectric generator improves for $\mu > 0$ and $\mu < 0$ a care must be taken to account for the thermal stresses. In this case, reducing the cross-sectional area for $\mu > 0$ may result in high stress intensities in the leg at operating temperatures while limiting the life of the device. Moreover, increasing temperature ratio enhances the efficiency. This is true for all shape parameters. This is more pronounced for $-2 \leqslant \mu \leqslant -1$ and $1 \leqslant \mu \leqslant 2$. This indicates that nonlinear effect of the shape parameter on the efficiency becomes considerable with increasing temperature ratio. Consequently, operating the thermoelectric power generator at high temperature ratio improves efficiency; however this improvement becomes considerable for the shape parameter in the range of $-2 \leqslant \mu \leqslant -1$ and $1 \leqslant \mu \leqslant 2$. Therefore trapezium shaped leg geometry results in better efficiency than that corresponding to the rectangular shape.

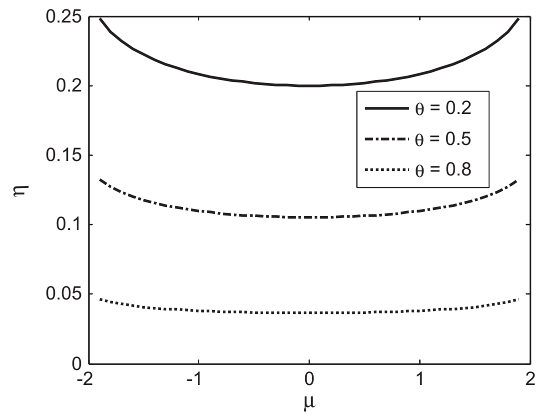

Fig. 3. Thermal efficiency variation with the shape parameter for different temperture ratios.

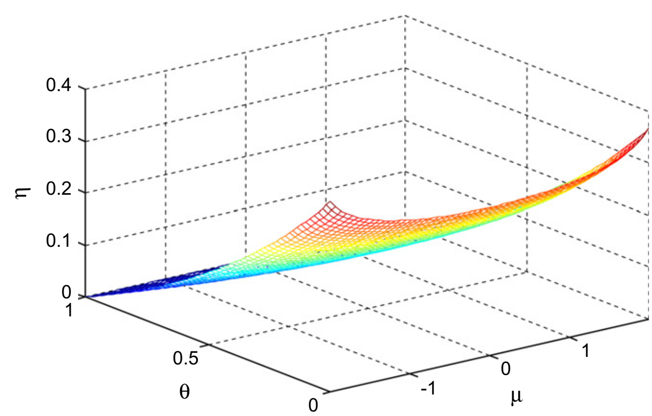

Fig. 4. Variation of efficiency with shape parameter and temperature ratio.

Fig. 5 shows thermoelectric generator output with the shape parameter. The influence of the shape parameter is notable on the thermoelectric power generation. This is more pronounced for low temperature ratio. The influence of shape parameter on the power generation is small for high temperature ratios, the power generation is also low for large temperature ratios. Consequently, the influence of the shape parameter on the power generation could not be observed clearly. On the other hand, for low temperature ratio, the influence of the shape parameter becomes considerable for both $-2 \leqslant \mu \leqslant -1$ and $1 \leqslant \mu \leqslant 2$. This is attributed to the value of the ratio of external load resistance (R_L) to the reference electrical resistance (R_o). Increasing R_L/R_o reduces the effect of the shape parameter on the power generation. This can be seen from Fig. 6, in which the thermoelectric power with the shape parameter is given for $R_L/R_o = 10$. Moreover, the power generation reduces with increasing or decreasing shape parameter, since the shape parameter enhances the overall electrical resistance of the thermoelectric generator (Eq. (12)). This results in low power generation (Eq. (25)). The power generated reaches its maximum for the shape parameter $\mu = 0$. This corresponds to rectangular leg geometry. Consequently, influence of the shape parameter could be minimized by increasing the external load parameter and the efficiency of the thermoelectric generator can be improved considerably for low temperature ratios.

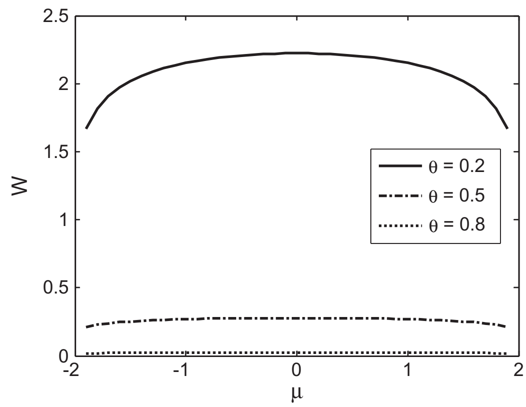

Fig. 5. Thermoelectric power generated as function of the shape parameter for different temperature ratios.

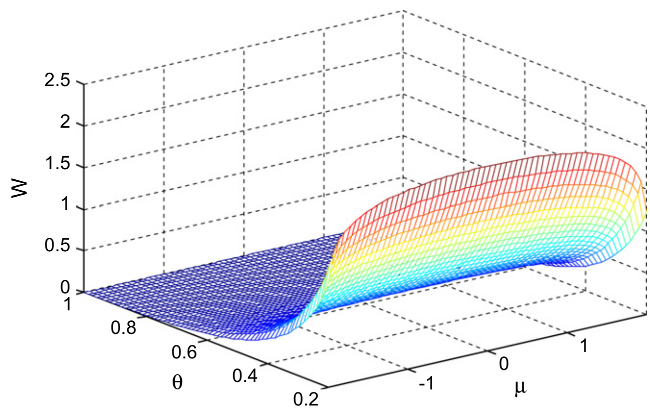

Fig. 6. Variation of thermoelectric power with shape parameter and temperature ratio.

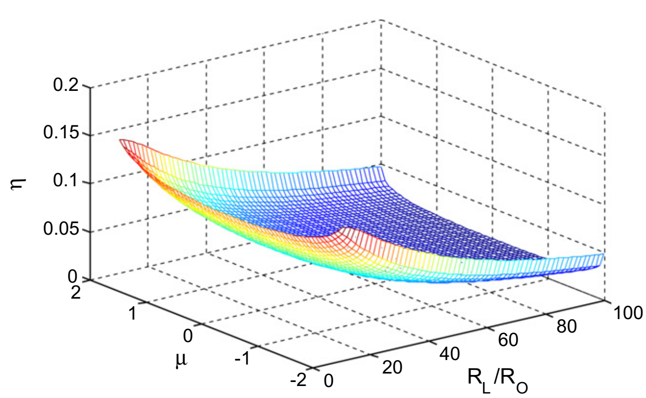

Fig. 7. Thermal efficiency of thermoelectric generator with the shape parameter and external load parameter.

Figs. 7 and 8 show three dimensional surface of the efficiency and the thermoelectric power generated for two R_L/R_o ratios. It is evident that increasing external load resistance reduces the efficiency and the power generated considerably. Therefore, selection of low external load resistance enhances both the efficiency and the power generation of the thermoelectric device. Moreover, the influence of the shape parameter on the efficiency and the power generation becomes notable for high temperatures (i.e. low temperature ratios). Therefore, the leg geometry modification only

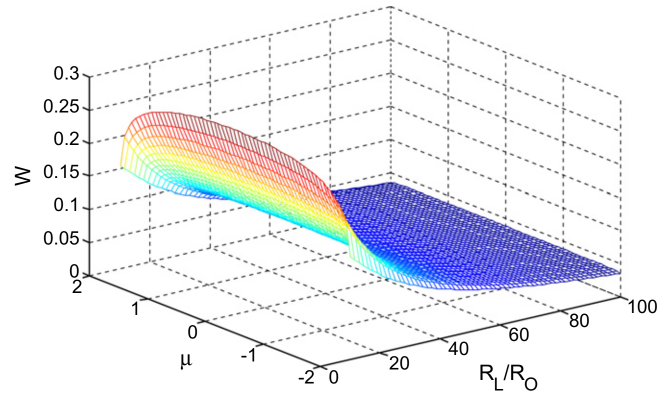

Fig. 8. Thermoelectric power generated as function of the shape parameter and external load parameter.

improves the efficiency when the device operates at low temperature ratios. Otherwise, this effect becomes negligible. The value of the power generation becomes maximum for the shape parameter for $\mu = 0$, which is true for all temperature ratios. Therefore, the shape parameter has an adverse affect on the power generation, but it has a favorable effect on the efficiency.

Fig. 9 shows the efficiency with the shape parameter for different values of the load parameter ratios. Efficiency increases for the shape parameter ranges $-2 \leqslant \mu \leqslant -1$ and $1 \leqslant \mu \leqslant 2$, which are

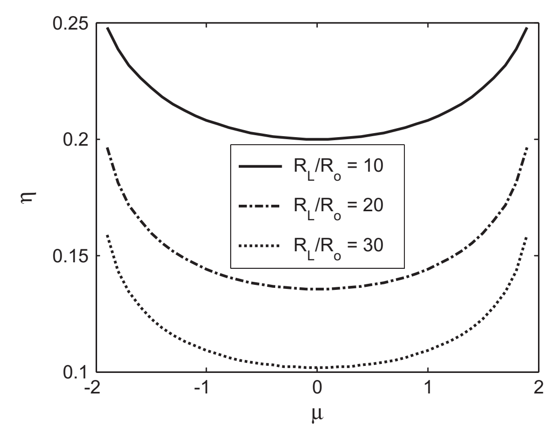

Fig. 9. Thermal efficiency variation with the shape parameter for different external load parameters.

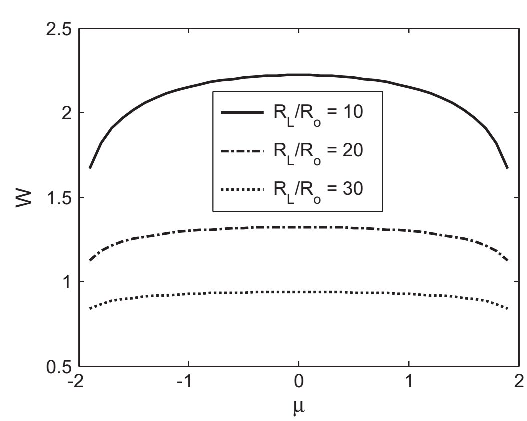

Fig. 10. Thermoelectric power generated as function of the shape parameter for different external load parameters.

similar to those shown in Fig. 3. This is associated with Eq. (13) in which, the efficiency is inversely related to the load parameter ratio. In this case, increasing external load resistance reduces the efficiency of the device, which is more pronounced for small values of the shape parameters. The efficiency reduces to its minimum regardless of the external load parameter ratio. Fig. 10 shows thermoelectric power generation with the shape parameter for different values of the load parameter ratio. The behavior of the thermoelectric power generation is similar to that is shown in Fig. 5. In this case, increasing load parameter ratio enhances the power generation, particularly for shape parameter $\mu = 0$. This behavior is attributed to Eq. (25), in which case, the shape parameter is inversely proportional to the thermoelectric power generation; further more, the influence of the load parameter ratio on this relation is more pronounced for $-2 \leqslant \mu \leqslant -1$ and $1 \leqslant \mu \leqslant 2$.

4. Conclusions

A theoretical analysis of thermoelectric power generator is carried out. The influence of the shape parameter, associated with the thermoelectric leg geometry, on the efficiency and power generation is formulated. The influence of the shape parameter on the efficiency and the power generation of the thermoelectric device are examined for different values of temperature ratio. It is found that the efficiency of the thermoelectric generator improves notably for certain ranges of the shape parameter, i.e. $-2 \leqslant \mu \leqslant -1$ and $1 \leqslant \mu \leqslant 2$. In this case, the leg geometry becomes a trapezium shape along the leg height. This is more pronounced for low temperature ratios. However, the power generation by the device reduces with increasing or decreasing shape parameter, which is more pronounced at low temperature ratio and the low external load resistance. Increasing external load resistance decreases the efficiency and the power generation. The influence of the shape parameter on the power generation becomes negligible as the external load resistance increase. Although the efficiency improves with increasing or decreasing shape parameter, the power generation reduces. Consequently, slight increase in the load resistance increases the device efficiency while slight reduction in the load resistance lowers the power generation. Therefore, when the high efficiency of the device is required decreasing or increasing in the shape parameter is favorable; however, when high power is required the shape parameter should be set to zero, which corresponds to the rectangular leg geometry.

Acknowledgments

The authors would like to acknowledge the support provided by the Deanship of Scientific Research at King Fahd University of Petroleum and Minerals (KFUPM), Dhahran, Saudi Arabia for this work under Research Grant RG1002.

References

[1] Rowe DM, editor. CRC handbook of thermoelectrics. Boca Raton, FL: RC; 1995.
[2] Rowe DM, editor. CRC handbook of thermoelectrics: macro to nano. Boca Raton, FL: RC; 2006.
[3] Rowe DM, editor. Thermoelectrics and its energy harvesting. CRC press; 2012.
[4] Ioffe A. Semiconductor thermoelements and thermoelectric cooling. London: Infosearch, ltd.; 1957.
[5] Goldsmid HJ. Applications of thermoelectricity. Butler & Tanner Ltd.; 1960.
[6] Egli PH. Thermoelectricity. New York: John Wiley & Sons, Inc.; 1960.
[7] Cadoff IB, Miller E, editors. Thermoelectric materials and devices, materials technology series, New York, 1960. Reinhold Publishing Cooperation. Lectures presented during the course on thermoelectric materials and devices sponsored by the Department of Metallurgical Engineering in cooperation with the office of special services to business and industry, New York, NY; June 1959 and 1960.
[8] Heikes RR, Roland W, Ure J. Thermoelectricity: science and engineering. New York: Interscience Publishers, Inc.; 1961.
[9] Levine SN, editor. Selected papers on new techniques for energy conversion. Dover Publications, Inc.; 1961.
[10] Sutton GW, editor. Direct energy conversion. vol. 3. Inter-University Electronics Series. McGraw-Hill Book Company; 1966.
[11] Tauc J. Photo and thermoelectric effects in semiconductors. New York: Pergamon press; 1962.
[12] Jaumot Jr. FE. Thermoelectricity. In: Marton L, Marton C, editors. Advances in electronics and electron physics. Academic Press, vol. 17. Advances in Electronics and Electron Physics; 1963. p. 207–43.
[13] Angrist SW. Direct energy conversion. Boston: Allyn and Bacon, Inc.: 150 Tremont Street; 1965.
[14] Harman TC, Honig JM. Thermoelectric and thermomagnetic effects and applications. New York: McGraw-Hill Book Company; 1967.
[15] Vatcharasathien N, Hirunlabh J, Khedari J, Daguenet M. Design and analysis of solar thermoelectric power generation system. Int J Sustain Energy 2005;24:115–27.
[16] Guo X, Xiao H, Yang S. Modeling, experimental study and optimization on low-temperature waste heat thermoelectric generator system. Appl Energy 2010;87:3131–6.
[17] Xiao H, Guo X, Yang C. Simulation analysis on thermoelectric generator system performance. In: 2008 Asia simulation conference – 7th International conference on system simulation and scientific computing, ICSC; 2008. p. 1183–87.
[18] Weinberg FJ, Rowe DM, Min G, Ronny PD. On thermoelectric power conversion from heat recirculating combustion systems. In: Proceedings of the combustion institute, twenty-ninth international symposium on combustion Hokkaido University Sapporo Japan; July 21–25, 2002.
[19] Crane DT, Bell LE. Progress towards maximizing the performance of a thermoelectric power generator. In: International conference on thermoelectrics, ICT, proceedings ICT06 – 25th international conference on thermoelectrics; 2006. p. 11–6.
[20] Freunek M, Muller M, Ungan T, Walker W, Reindl LM. New physical model for thermoelectric generators. J Electron Mater 2009;38:1214–20.
[21] Chen L, Meng F, Sun F. A novel configuration and performance for a two-stage thermoelectric heat pump system driven by a two-stage thermoelectric generator. Proc Institut Mech Eng A J Power Energy 2009;223:329–39.
[22] Suzuki R, Tanaka D. Mathematical simulation of thermoelectric power generator with the multi-panels. J Power Sources 2003;122:201–9.
[23] Amatya R, Ram RJ. Solar thermoelectric generator for micropower applications. J Electron Mater 2010;39:1735–40.
[24] Yamashita O. Effect of linear temperature dependence of thermoelectric properties on energy conversion efficiency. Energy Conver Manage 2008;49:3163–9.
[25] Yilbas BS, Sahin AZ. Thermoelectric device and optimum external load parameter and slenderness ratio. Energy 2010;35:5380–4.
[26] Yamashita O. Effect of linear and non-linear components in the temperature dependences of thermoelectric properties on the energy conversion efficiency. Energy Conver Manage 2009;50:1968–75.
[27] James WS. Optimal design of small ΔT thermoelectric generation systems. Energy Conver Manage 2001;42:709–20.
[28] Domenicali CA. Irreversible thermodynamics of thermoelectricity. Rev Modern Phys 1954;26:237–75.
[29] Goupil C et al. Thermodynamics of thermoelectric phenomena and applications. Entropy 2011;13:1481–517.
[30] James AB. Solutions to the differential equations describing the temperature distribution, thermal efficiency, and power output of a thermoelectric element with variable properties and cross sectional area. Adv Energy Conver 1962;2:219–30.
[31] Clingman WH. Entropy production and optimum device design. Adv Energy Conver 1961;1:61–79.
[32] Landecker K. Some aspects of the performance of refrigerating thermojunctions with radial flow of current. J Appl Phys 1976;47(5):1846–51.
[33] Landecker K. On power-generating thermojunctions with radial flow of current. Solar Energy 1977;19(5):439–43.
[34] Landecker K. Heat transport in coaxial thermoelectric disks with radial flow of current. J Appl Phys 1978;49(9):4939–41.
[35] Gao M. Thermoelectric module design theories. In: David Mike Rowe, editor. CRC handbook of thermoelectrics: macro to nano. Boca Raton, FL: Taylor and Francis; 2006 [chapter 11].
[36] Gao M, Rowe DM. Ring-structured thermoelectric module. Semicond Sci Technol 2007;22(8):880.
[37] Riffat SB, Qiu GQ. Design and characterization of a cylindrical, water-cooled heat sink for thermoelectric air-conditioners. Int J Energy Res 2006;30:67–80.
[38] Semenyuk VA. Efficiency of cooling thermoelectric elements of arbitrary shape. J Eng Phys Thermophys 1977;32(2):196–200.
[39] Antonio A, Jorge V, Rafael P. Performance analysis of thermoelectric pellets with non-constant cross sections. In: Proceedings of the 7th European workshop on thermoelectrics, Paper #26. Pamplona, Spain; October 2002.
[40] Thacher EF. Shapes which maximise thermoelectric generator efficiency. In: Proc 4th international conference on thermoelectric energy conversion, Arlington, Texas, USA; 1982. p. 67–74.
[41] Bejan A, Lorente S. Design with constructal theory. Hoboken: Wiley; 2008.
[42] Goncalves LM, Couto C, Alpuim P, Rowe DM, Correia JH. Thermoelectric properties of Bi_2Te_3/Sb_2Te_3 thin films. Mater Sci Fórum 2006;514–516:156–60.

[43] Böttner H, Nurnus J, Gavrikov A, Kühner G, Jägle M, Künzel C, et al. New thermoelectric components using microsystem technologies. J Microelectromech Syst 2004;3:414.

[44] Giani A, Boulouz A, Pascal-Delannoy F, Foucaran A, Charles E, Boyer A. Growth of Bi_2Te_3 and Sb_2Te_3 thin films by MOCVD. Mater Sci Eng 1999;B64:19–24.

[45] Zou H, Rowe DM, Williams SGK. Peltier effect in a co-evaporated Sb_2Te_3(P) – Bi_2Te_3(N) thin film thermocouple. Thin Solid Films 2002;408:270.

[46] Lim JR, Snyder GJ, Huang CK, Herman JA, Ryanand MA, Fleurial JP. Thermoelectric microdevice fabrication process and evaluation at the jet propulsion laboratory, ICT; 2002.

[47] Foucaran A. Flash evaporated layers of (Bi_2Te_3–Bi_2Se_3)(N) and (Bi_2Te_3–Sb_2Te_3)(P). Mater Sci Eng 1998;B52:154–61.

[48] Sclar N. Thermoelectric infrared detertor array. US Patent no. 4,558,342; 1985.